In the Proceedings of the Second Asia-Pacific Workshop on Near-field Optics, Beijing, China, October 20-23, 1999.

NEAR-FIELD SCANNING OPTICAL MICROSCOPY OF ELECTROMIGRATION IN YBCO

Suzanne Huerth, Michael Taylor, Michael Paesler, Hans Hallen
North Carolina State University, Raleigh NC 27695

We have used a near-field scanning optical microscope (NSOM) to both electromigrate oxygen in $YBa_2Cu_3O_{7-\delta}$ (YBCO), and to image the results of the electromigration with nanometer resolution. The metallic aperture is used as a one electrode for electromigration. Reflectance in the visible portion of the spectrum is used as a measure of local oxygen concentration. This reflectance depends on oxygen concentration and is therefore a measure of the YBCO's superconducting properties.

1 Introduction

The near-field scanning optical microscope (NSOM) allows optical studies with imaging and processing capabilities below the Abbe resolution limit. It has been used extensively for materials analysis,[1] spectroscopy,[2,3] and electron-hole recombination time imaging.[4] Since the NSOM utilizes a metal clad probe, it may be used to induce electromigration on the nanometer scale. The metal clad probe acts as an electrode, producing a tunneling current when a voltage is applied to the sample and the lateral force feedback is adjusted to bring the sample closer to the probe. Current density estimates for the region surrounding the tunnel contact suggest that the current density is too low to induce electromigration over a significant area. However, the energy of the tunnel-injected electrons is much higher than that used in prior experiments. Thus, the applied voltage becomes the dominating variable in electromigration. The same microscope may subsequently be used to image the effects of the NSOM-induced electromigration through the known variation in $YBa_2Cu_3O_{7-\delta,}$ (YBCO) reflectivity with oxygen concentration.

Electromigration of oxygen in YBCO is important for superconducting device fabrication and consequently has been carefully studied.[5-7] In such applications it is desirable to enhance the quality of devices by increasing the critical current of the

Josephson junctions. Storage lifetime and reliability issues also depend upon the oxygen stability. In a number of studies, the superconducting current versus applied voltage is measured before and after electromigration under various conditions. For current densities of 3-5MA/cm^2 at room temperature, improved junction critical current results. Degradation sets in at a higher current density or longer times. No changes in the superconducting properties were observed upon attempts at electromigration below the superconducting transition temperature.[5] Reversal of the effects of the electromigration can be realized, at least in part, by heating the samples in an oxygen atmosphere.[6]

In these prior studies, electromigration was investigated by determining changes in the superconducting properties on a macroscopic scale. A deeper understanding of the effects of electromigration might be developed if a microscopic study of the migration of oxygen were undertaken. In the present paper, we localize the electromigration of oxygen by using a near-field scanning optical microscope (NSOM) metal clad probe as one of the electrodes. The effect is then studied by observing changes in the reflectance due to induced differences in oxygen concentration. Advantages of this method include the ability to locate the probe for electromigration either within a grain or near a grain boundary, and the ability to control both the energy and number of injected electrons.

Changes in the index of refraction can be studied by monitoring the intensity of light reflected from a surface. Several groups have studied the optical properties of YBCO in this manner.[8-10] Kamaras et al[10] found that the reflectivity of YBCO decreases with oxygen concentration for green light. They also observed a decrease in reflectance at higher frequencies. NSOM images of aged and electromigrated samples are consistent with prediction based on these data.

The rather complex physics of electromigration has been modeled.[11-15] Electromigration is essentially momentum transfer from moving electrons in the "electron wind" to oxygen atoms in the lattice. The force due to the electron wind is $F \sim J\sigma m\Delta\upsilon N$. For YBCO with a current density of 5MA/cm^2, this force is approximately 10^{-9} dynes. YBCO is a tetragonal lattice, and the oxygen moves in the Cu(1) planes.[16] At room temperature, the oxygen is stable in the lattice[16], and thus any movement is due to an applied force. The oxygen can electromigrate out of the sample as well as to another lattice site. Oxygen migration can be imaged with a near-field scanning optical microscope, where the changes in reflectivity are indications of differences in the oxygen concentration.

2 Methods

The sample was imaged using a near-field scanning optical microscope in reflection mode. A standard NSOM consists of a shear force regulation, a scanning mechanism, illumination, and collection optics. The sample is carbon-taped to an extender tube mounted on a piezoelectric scanner tube. Shear force regulation keeps the tip-sample distance constant during scanning. In our setup, the shear force is detected using the tuning fork method pioneered by Karrai and Grober[17]. The metal clad probe is glued to the tuning fork and the changes in the resonance frequency of the tuning fork are used to maintain feedback with a tip-sample distance of approximately 8nm.

Monochromatic light is couple into the fiber and the reflected light focused by a 0.45NA lens onto a photodiode. The preamplified signal is low-pass filtered with analog and digital methods as it is read into the computer. The optical image and topographic image are collected simultaneously. The metal clad probe is fabricated with the heat and pull method followed by evaporative coating. A modified micro-pipette puller is used to heat the stripped fiber with a CO2 laser while pulling on the ends of the fiber. The tips are radiatively cooled by a LN2 cold plate as they are rotated during coating, so that the grains are smaller and hence the aperture smoother. The shroud also improves Al quality by pumping water vapor. A layer of aluminum approximately 500nm is applied.

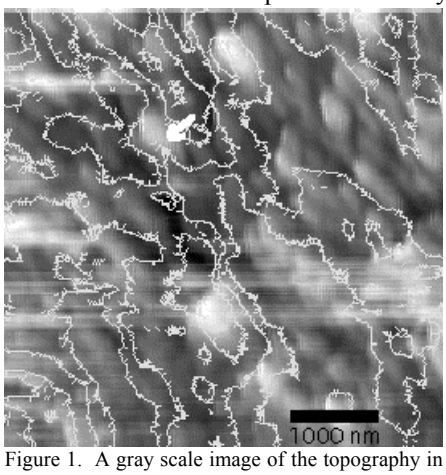

Figure 1. A gray scale image of the topography in a 5 µm by 5 µm region (150 nm vertical range, white higher) is overlayed with a contour plot of the simultaneously acquired optical data (range 10 nW, white lower reflectivity, higher oxygen content) before electromigration. The tick marks on the contours point towards lower oxygen content. Note the correlation between the oxygen concentration and the grains. The arrow points towards the region of subsequent electromigration.

Monochromatic light at 514 and 488 nm from a tunable argon laser was injected into the fiber that was terminated in the metal clad probe. An image was obtained for each wavelength before and after each electromigration.

Electromigration was induced with a negative voltage applied to the sample and using the probe as a tunneling electrode. To allow tunneling, the shear force regulation level was reduced, causing the sample to approach the tip. Probe current was monitored during this period with a current preamplifier. Once the current reached the desired level, or the tip was less than 1nm from the sample, the probe was stopped and, except for feedback dithering, held in this

position for a set amount of time. The time varied from 36 minutes to 8 hours and the voltage ranged from –1 volt to –3 volts. The applied force for electromigration due to the electron wind immediately underneath the tip is approximately 2.5 x 10^{-8} dynes or 20 times the force calculated for macroscopic electromigration.

3 Results

We imaged two industrially grown (Conductus, Inc.) samples that had been aged one year under low moisture conditions at room temperature. The samples were imaged before and after electromigration. The 'before' scans showed that the oxygen content at the surface of different grains varied, although it tended to remain fairly constant within a grain. Of particular note is that grains that project above the average surface height tend to have lower oxygen content than their lower neighbors. This can be explained by the anisotropic diffusivity of oxygen -- it tends to move more easily in the ab planes than along the c-direction. The oxygen does not need to move far in the projecting grains before escaping from the sample. The relation can be seen in Figure 1, which shows a gray scale topography with the optical data overlayed as contours. As expected, the correlation between height and oxygen content is not perfect, rather the changes in oxygen concentration occur at grain boundaries. Note that this is not a topographic artifact, since artifacts are localized at topographic changes, whereas these data show consistency across the grains. The size of the grains was approximately 300-500nm in length with a height of 40-80nm

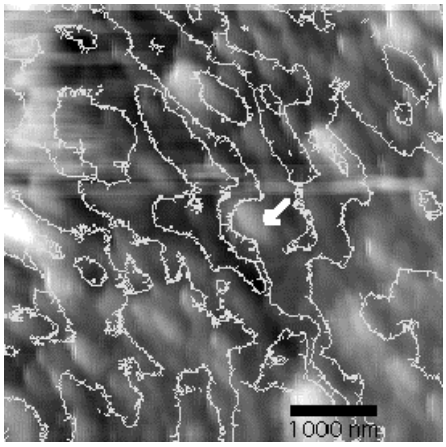

Figure 2. An 'after electromigration' gray scale image of the topography in a 5 µm by 5 µm region (150 nm vertical range, white higher) is overlayed with a contour plot of the simultaneously acquired optical data (range 10 nW, white lower reflectivity, higher oxygen content). The tick marks on the contours point towards lower oxygen content. Note the correlation between the oxygen concentration and the grains. The arrow indicates the major paths of oxygen flow.

Electromigration was obtained by applying -1 volt to the sample and bringing the sample to the tip until the tunnel current reached 2nA. The system was left in this state for 36 minutes. Ten micron square images were taken with 488 and 514nm monochromatic light. We used a two-dimensional correlation function between the topographic images to determine a 0.267 µm/hr drift (correlation of the optical images

gave the same drift to within one pixel). We used this drift value to shift the optical data for comparison. There was a noticeable 0.22 μm^2 effect. A comparison of the optical and topographic images indicated that the oxygen had moved from the bulk to a surface projecting grain. This can be seen in Figure 2, in which the topographic image is overlayed with contour lines from the corresponding optical image. The shifting contours are indicative of the motion of oxygen.

We changed the sample and the tip and repeated the experiment with a voltage of -3 volts for 8 hours and a tunnel current of 3nA. Again, we determined the drift, then compared the before and after optical images, finding a 0.70 μm^2 effect.

The size of the effect should depend upon the region for which the force is sufficient to move oxygen atoms. The contribution due to the current density falls as the current spreads out, eventually dropping as 1/distance for a thin film. A prediction of the size that the electromigration should effect using current density requirements from the literature yields a radius much smaller than we observe. We inject the electrons with a higher momentum, however, due to the increased local potential drop. It is likely that this voltage effect plays a major role in this process, as it has in other low-energy-electron-induced processes.[18] In that study, the size limitation was found to be limited by growth dynamics, and eventually the grain size. The figures support a similar conclusion here.

4 Conclusions

We have shown that a near-field scanning optical microscope can be used to both induce and image the effects of electromigration in YBCO. The images showed nanometric variations in the oxygen concentration with a correlation to the grain structure. We found that the size of the effect due to electromigration is not strictly a function of the current density, but depends on the velocity of the electrons, which relates to the voltage used, and that there is a limit to the size of the effect. Further studies will provide understanding of the physical mechanism of local electromigration of oxygen in YBCO.
This work was supported by the Office of Naval Research through grant N00014-98-1-0228.

References

1. H. D. Hallen, A. La Rosa, and C.L. Jahncke, "Near-field scanning optical microscopy and spectroscopy for semiconductor characterization," Physica Status Solidi (a) **152**, 257-268 (1995).
2. C.L. Jahncke, M. A. Paesler, and H.D. Hallen, "Raman imaging with near-field scanning optical microscopy," Appl. Phys. Lett. **67**, (17), 2483-2485 (1995).
3. C.L. Jahncke and H. D. Hallen."Near-field Raman Spectra: surface enhancement, z-polarization, fiber Raman background, and Rayleigh scattering", 9th annual meeting of IEEE Lasers and Electro-Optics Society (LEOS) 96 conference proceedings volume **1**, pp. 176-177.
4. A.H. La Rosa, B. I. Yakobson, H.D. Hallen, "Optical imaging of carrier dynamics with sub- wavelength resolution," Appl. Phys. Lett. **70** (13), 1656-1658 (1997).
5. J. B. Bulman and J. M. Murduck; "Modification of Step-Edge Grain Boundary Josephson Junctions by Electromigration"; IEEE Transactions on Applied Superconductivity 5 (2), pp. 2813-2815 (1995).
1. B. H. Moeckly, D. K. Lathrop, and R. A. Buhrman; "Electromigration study of oxygen disorder and grain-boundary effects in $YBa_2Cu_3O_{7-\delta}$ thin films"; Phys. Rev. B 47 (1), pp. 400-417 (1993).
7. K. G. Rajan, P. Parameswaran, J. Janaki, and T. S. Radhakrishnan; "Electromigration of oxygen in $YBa_2Cu_3O_{7-\_}$ "; J. Phys. D: Appl. Phys. **23**, pp. 694-697 (1990)
8. P.E. Sulewski et al; "Free-carrier dynamics in the normal state of sintered $YBa_2Cu_3O_{7-\_}$ "; Phys. Rev. B **36** (4), pp. 2357-2360 (1987).
9. G. Zhao, Y. Xu, W.Y. Ching, K. W. Wong; "Theoretical Calculation of Optical Properties of Y-Ba-Cu-O Superconductors"; Phys. Rev. B, **36** pp.7203 (1987).
10. K. Kamaras et al; "Excitonic Absorption and Superconductivity in $YBa_2Cu_3O_{7-\delta}$"; Phys. Rev. Lett. **59** (8), pp. 919-922 (1987).
11. K. P. Rodbell, M.V. Rodriguez, and P. J. Ficalora; "The kinetics of electromigration"; J. Appl. Phys. **61** (8), pp. 2844-2848 (1986).
12. M.L. Dreyer, K.Y. Fu, and C.J. Varkar; "An electromigration model that includes the effects of microstructure and temperature on mass transport"; J. Appl. Phys. **73** (10), pp. 4894-4902 (1993).
13. K. Hinode, T. Furusawa, and Y. Homma; "Dependence of electromigration damage on current density"; J. Appl. Phys. **74** (1), pp.201-206 (1993).
14. H. Boularot and R. M. Bradley; "Mean-field theory of electromigration-induced void drift and coalescence in metal thin films"; J. Appl. Phys. **80** (2), pp. 756-761 (1996).
15. J. R. Lloyd; "Electromigration in thin film conductors"; Semicond. Sci. Technol. **12,** pp. 117-1185 (1997).
16. J. B. Goodenough and A. Manthiram; "The Role of Oxygen in $YBa_2Cu_3O_{7-\delta}$ "; Proceedings of the IX Winter meeting on Low Temperature Physcis: *High Temperature Superconductors* (1988).
17. K. Karrai and R. Grober; "Piezoelectric tuning fork tip-sample distance control for near field optical microscopes"; Ultramicroscopy **61**, pp. 197-205 (1995).
18. H.D. Hallen, A. Fernandez, T. Huang, R.A. Buhrman, and J. Silcox, "Hot electron interactions at the passivated gold-silicon interface," Phys. Rev. Lett. **69**, 2931 (1992).